Am J Transl Res 2013;5(6):608-621
www.ajtr.org /ISSN:1943-8141/AJTR1308003

Original Article

Distinct subcellular patterns of neprilysin protein and activity in the brains of Alzheimer's disease patients, transgenic mice and cultured human neuronal cells

Li Zhou[1*], Chunsheng Wei[1*], Wei Huang[4], David A Bennett[2], Dennis W Dickson[3], Rui Wang[1,4], Dengshun Wang[4]

[1]Shanghai Key Laboratory of New Drug Design, School of Pharmacy, East China University of Science and Technology, Shanghai 200237, China; [2]Rush Alzheimer's Disease Center, Rush University Medical Center, Chicago, IL, USA; [3]Department of Pathology (Neuropathology) and Neuroscience, Mayo Clinic College of Medicine, Jacksonville, FL 32224, USA; [4]Department of Pathology and Laboratory Medicine, School of Medicine and Public Health, University of Wisconsin, Madison, Wisconsin, USA. [*]Equal contributors.

Received August 8, 2013; Accepted August 27, 2013; Epub September 25, 2013; Published September 30, 2013

Abstract: We investigated the subcellular distribution of NEP protein and activity in brains of human individuals with no cognitive impairment (NCI), mild cognitive impairment (MCI) and AD dementia, as well as double transgenic mice and human neuronal cell line treated with Aβ and 4-hydroxy-2-nonenal (HNE). Total cortical neuronal-related NEP was significantly increased in MCI compared to NCI brains. NeuN was decreased in both MCI and AD, consistent with neuronal loss occurring in MCI and AD. Negative relationship between NEP protein and NeuN in MCI brains, and positive correlation between NEP and pan-cadherin in NCI and MCI brains, suggesting the increased NEP expression in NCI and MCI might be due to membrane associated NEP in non-neuronal cells. In subcellular extracts, NEP protein decreased in cytoplasmic fractions in MCI and AD, but increased in membrane fractions, with a significant increase in the membrane/cytoplasmic ratio of NEP protein in AD brains. By contrast, NEP activity was decreased in AD. Similar results were observed in AD-mimic transgenic mice. Studies of SH-SY5Y neuroblastoma showed an up-regulation of NEP protein in the cytoplasmic compartment induced by HNE and Aβ; however, NEP activity decreased in cytoplasmic fractions. Activity of NEP in membrane fractions increased at 48 hours and then significantly decreased after treatment with HNE and Aβ. The cytoplasmic/membrane ratio of NEP protein increased at 24 hours and then decreased in both HNE and Aβ treated cells. Both HNE and Aβ up-regulate NEP expression, but NEP enzyme activity did not show the same increase, possibly indicating immature cytoplasmic NEP is less active than membrane associated NEP. These observations indicate that modulation of NEP protein levels and its subcellular location influence the net proteolytic activity and this complex association might participate in deficiency of Aβ degradation that is associated with amyloid deposition in AD.

Keywords: Alzheimer's disease, amyloid-β, Aβ degrading enzymes, neprilysin, subcellular compartments, Aβ clearance

Introduction

Alzheimer's disease (AD) is characterized by extracellular β-amyloid (Aβ) deposits in the form of senile plaques and cerebral amyloid angiopathy, as well as intracellular neurofibrillary tangles composed of hyperphosphorylated microtubule associated protein tau [1]. Accumulation of Aβ, a physiological peptide in the brain, is thought to be a triggering event in the pathological cascade of AD [1]. The steady-state level of Aβ is determined through a balance between the anabolic and catabolic activities. Excessive Aβ deposition in AD brains is related to the dynamic interaction of its production and degradation. Although overproduction of Aβ is a crucial factor in approximately 5-10% of AD cases associated with autosomal dominant mutations in amyloid precursor protein (APP) [2, 3], presenilin 1 (*PSEN1*) [4], or *PSEN2* [5, 6], there is little evidence of Aβ overproduction in aging and sporadic AD, where the cause of Aβ deposition remains uncertain. Thus, defining the mechanisms and cellular pathways of

Aβ catabolism remain important research objectives.

Neprilysin (NEP), a 97 kDa type II membrane-bound zinc metalloendopeptidase, is ubiquitously expressed by neurons [7]. It was originally identified in the renal brush border, but subsequently found in brain as a key neuropeptide-degrading enzyme (also known as enkephalinase, substance P-degrading enzyme, neutral endopeptidase, EC 3.4.24.11, and CD10), although expressed at much lower levels in the brain than in the kidney [8-11].

Several lines of evidence implicate NEP as the most potent Aβ-degrading enzyme in the brain and one that can degrade not only monomeric forms of Aβ, but also more toxic Aβ oligomers [12]. It was demonstrated that NEP knockout mice have increased levels of Aβ peptides in the brain and that administration of the NEP inhibitor thiorphan to rats led to increased levels of Aβ [8, 13-15]. In contrast, over-expression of NEP reduced Aβ levels in a dose-dependent manner [16, 17], protected neurons from Aβ toxicity *in vitro* [18], reversed amyloid-like pathology and improved animal behavior *in vivo* [13, 16, 19, 20]. NEP has been shown to be selectively decreased in AD brains, but not in pathological aging, which is associated with high levels of amyloid deposition without concomitant neurofibrillary degeneration [21]. Consistent with the increase in Aβ levels observed during aging and in AD, studies from others [20, 22-24] and us [21, 25] indicated that expression of NEP in the brain decreases not only in aged rodents, but also in early stages of AD. Decreases in NEP correlated with Aβ accumulation and with clinical diagnosis [26].

NEP is a cell-surface ectoenzyme with a large extracellular domain containing the catalytic site, which is localized in a cavity that allows access to peptides containing up to 50 amino acids [27]. Recent evidence indicates that NEP is detected in lipid rafts [28-30], a cellular domain in which Aβ generation could occur [31, 32]. The evidence that both extracellular and cell-associated Aβ levels are reduced by over-expression of NEP in primary cortical neurons [33] suggests that NEP may degrade Aβ through a secretory pathway or possibly on the cell surface. A study with neurons expressing NEP chimeric proteins containing various subcellular compartment-targeting domains indicated that NEP in subcellular compartments had different catalytic activity [34]. Different intracellular compartments may be involved in the metabolism of distinct pools of Aβ (Aβ40 and Aβ42) that are retained or recycled intracellularly or secreted extracellularly [34]. We found in a previous study of SH-SY5Y human neuroblastoma cell line that expression of NEP mRNA and protein were up-regulated after Aβ treatment, but that NEP activity was significantly lower compared with NEP protein level [35]. Therefore, we speculated that the pattern of subcellular expression of NEP might differ in AD compared to controls and that this might contribute to abnormal Aβ catabolism and extracellular deposition of Aβ. Little work has been carried out on subcellular expression patterns of NEP and its enzymatic activity in brains of individuals with a range of AD pathology. Our objective was to make such assessment with the intent that this information might shed light on the pathogenesis of Aβ deposition in AD and possible lead to new therapeutic targets.

In this study, we investigated the subcellular distribution of NEP in the brains of individuals with NCI, MCI and AD, as well as in transgenic mice that develop Aβ in a predictable age-dependent manner. We complemented *in vivo* studies with *in vitro* studies of cultured human neuroblastoma SH-SY5Y cells treated with an inducer of oxidative stress, 4-hydroxy-2-nonenal (HNE), and with exogenous Aβ peptides.

Material and methods

Chemicals and reagents

Synthetic human Aβ1-42 was purchased from BACHEM (Torrance, CA). HNE was obtained from AG Scientific, Inc. (San Diego, CA). Mac-R-P-P-G-F-S-A-F-K (Dnp)-OH Fluorogenic Peptide Substrate V was purchased from R&D Systems, Inc. (Minneapolis, MN). Subcellular protein fractionation kits were purchased from Thermo Scientific (Rockford, IL). Human neprilysin ELISA kits were from R&D. Other general chemicals and reagents were from Fisher Scientific (Waltham, MA).

Case and clinical features data

Frozen frontal cortex from 6 NCI, 10 MCI and 12 AD were obtained from participants in the Religious Orders Study of the Rush Alzheimer

Disease Center (P30AG10161) [36]. All individuals had undergone a uniform structured clinical evaluation that included a medical history, neurologic examination, neuropsychological performance testing, and diagnostic classification for dementia and AD, and MCI; NCI referred to those individuals without dementia or MCI.

Animals

APPswe/PS1dE9 double-transgenic mice, expressing a chimeric mouse/human amyloid precursor protein (Mo/HuAPP695swe) and human mutant presenilin 1 (PS1-dE9), as well as wild-type C57 mice were obtained from Jackson Laboratory. Animals were housed at a temperature of 20-25°C, relative humidity of 50-60%, and a 12:12 hour reverse light: dark cycle environment with free access to food and water. All experimental procedures conformed to the guidelines of Care and Use of Laboratory Animals of China for animal experimentation.

Sample preparation and subcellular fractionation

Human brain samples were weighted, cut into small pieces in ice cold PBS (0.1 M sodium phosphate, 0.15 M sodium chloride; pH 7.2), and centrifuged at 500 xg for 5 min at 4°C. Supernatants were discarded, and the pellet was dissolved in 300 µl cytoplasmic extraction buffer (CEB), homogenized on ice, incubated for 10 min, and then centrifuged at 500 xg for 10 min. Supernatants (cytoplasmic extracts) were transferred to a new tube and 150 µl membrane extraction buffer (MEM) was added to the pellets, vortexed strongly for 5 seconds, incubated for 10 min on ice, then centrifuged at 3,000 xg for 10 min. The protein extracts were transferred to tubes and stored at -80°C until usage.

Cell culture and treatments with HNE and Aβ peptide

SH-SY5Y neuroblastoma cells, obtained from the American Type Culture Collection (ATCC), were maintained in a humidified atmosphere of 95% air and 5% CO_2 at 37°C. Cells were seeded into plates or dishes in DMEM/F12 (1:1) medium, supplemented with 10% (v/v) fetal bovine serum (FBS), 100 U/ml penicillin and 100 µg/ml streptomycin. SHSY5Y cells were seeded into 100 mm dishes at a density of 2 x 10^4 cells per ml. Experiments were carried out 24-48 h after cells were seeded. Different concentrations of HNE (dissolved in 3% DMSO) or Aβ (dissolved in 0.4% DMSO) were added to the cultures 24-72 h before harvest. Final concentration of DMSO in medium was < 0.003%. As a control, media (with same concentrations of DMSO) were added to the cells.

For subcellular fractionation, cells were harvested with trypsin-EDTA and then centrifuged at 500 xg for 5 min. The cells were washed by suspending the cell pellet with ice-cold PBS, transferred to 1.5 ml microcentrifuge tubes at 1-10 x 10^6 ml, and pelleted by centrifugation at 500 xg for 2-3 min. The supernatant was discarded and the cell pellet was re-suspended in ice-cold CEB containing protease inhibitors, before subcellular protein extraction as described above.

NEP protein and NEP enzymatic activity measurements

Cytoplasmic and membrane samples from brain tissues and cells treated with vehicles, HNE or Aβ were assayed for NEP protein level with a sandwich enzyme immunosorbant assay (ELISA) and for NEP enzyme activity with an immunocapture-based enzyme assay.

NEP protein level was measured with the NEP DuoSet® ELISA kit (R&D). Sandwich ELISA assay of NEP was performed according to the protocol provided by manufacturer. Standard curves were produced from serial dilutions of recombinant human NEP.

For immunocapture-based specific NEP activity measurements, 96-well high affinity binding ELISA plates (BD Bioscience, San Jose, CA) were coated with 100 µl of NEP capture antibody (goat anti-human, 1.6 µg/ml) diluted in PBS (137 mM NaCl, 2.7 mM KCl, 8.1 mM Na_2HPO_4, 1.5 mM KH_2PO_4, pH 7.2) and incubated for 18 h at room temperature. The plates were washed 3 times with PBS containing 0.05% tween-20. After 60 min blocking with PBS containing 1% BSA fraction V, 100 µl of standards or supernatants were added and incubated at 4°C overnight. After 3 washes, the fluorogenic peptide (10 µM) diluted in 100 mM Tris-HCl pH 7.5, 50 mM NaCl and 10 µM $ZnCl_2$ was added and incubated at 37°C in dark.

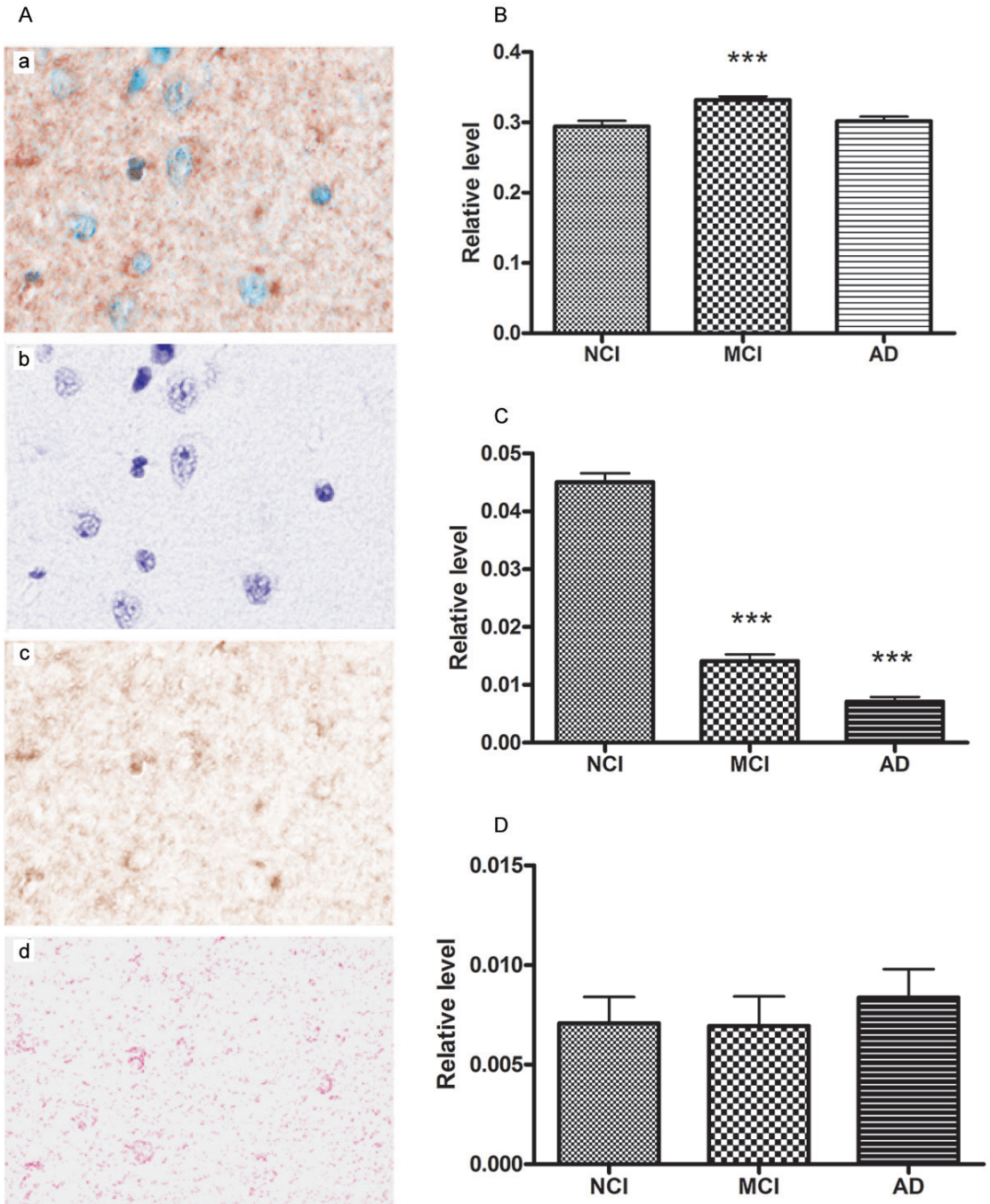

Figure 1. The relative levels of NEP, NeuN and Pan-cadherin in NCI, MCI and AD cortex. Brain slides from NCI, MCI and AD cortex were immunostained for NEP, NeuN and pan-cadherin followed by quantitative analysis using Art Imaging Systems Vectra™. A: The representative photos from the Nuance analysis. B: NEP; C: NeuN; D: Pan-cadherin. The data are expressed as mean ± SEM. ***$p < 0.01$ vs NCI control.

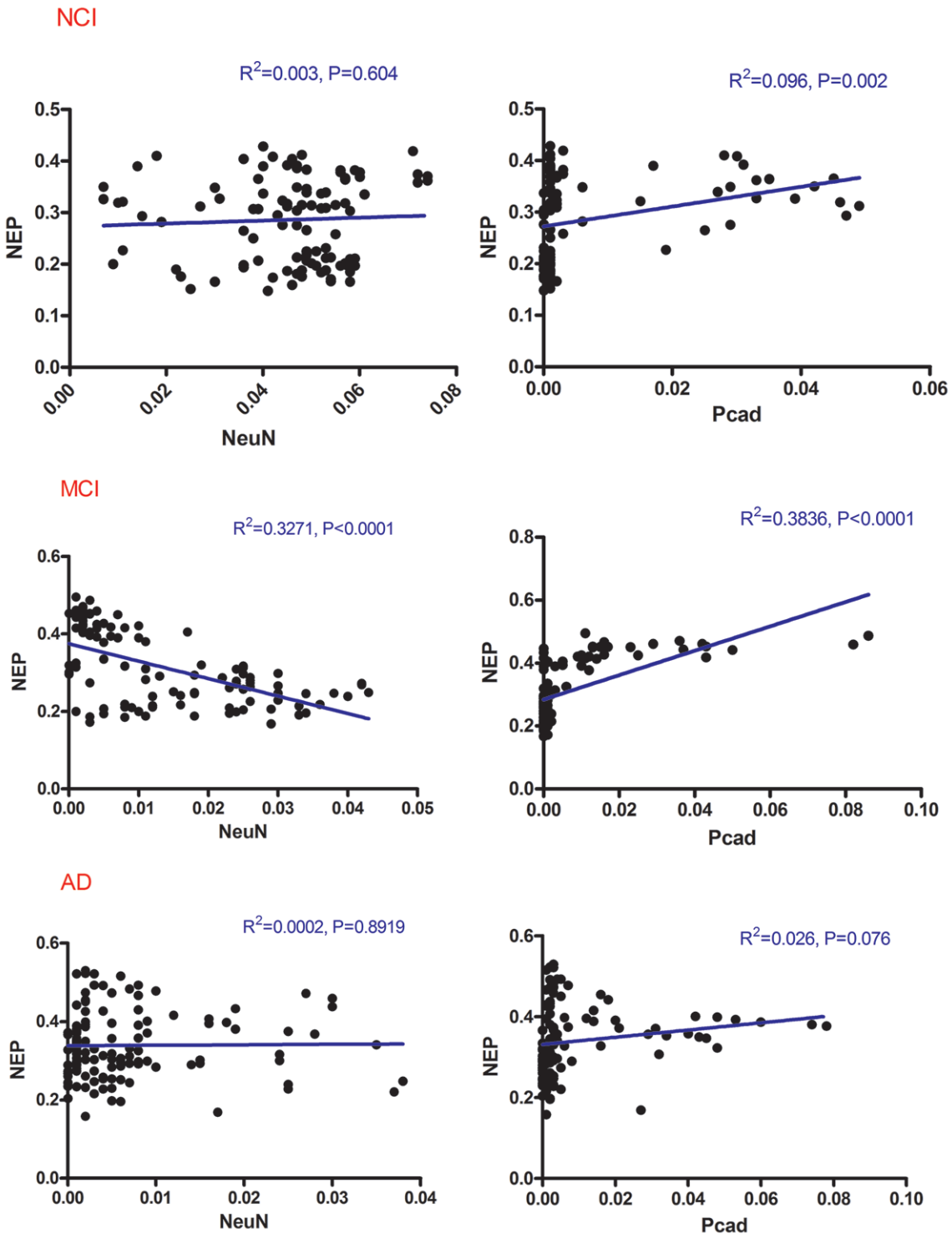

Figure 2. Correlation analysis of NEP/NeuN and NEP/pan-cadherin pixel density. A significant negative correlation between NEP and NeuN was observed only in MCI brains (R^2 = 0.3271, P < 0.0001). Positive correlation between NEP and pan-cadherin was observed in both NCI (R^2 = 0.096, P = 0.002) and MCI (R^2 = 0.3836, P < 0.0001).

Fluorescent readings were taken after 60 min. Control wells included in each plate contained PBS and fluorogenic peptide without cell supernatants.

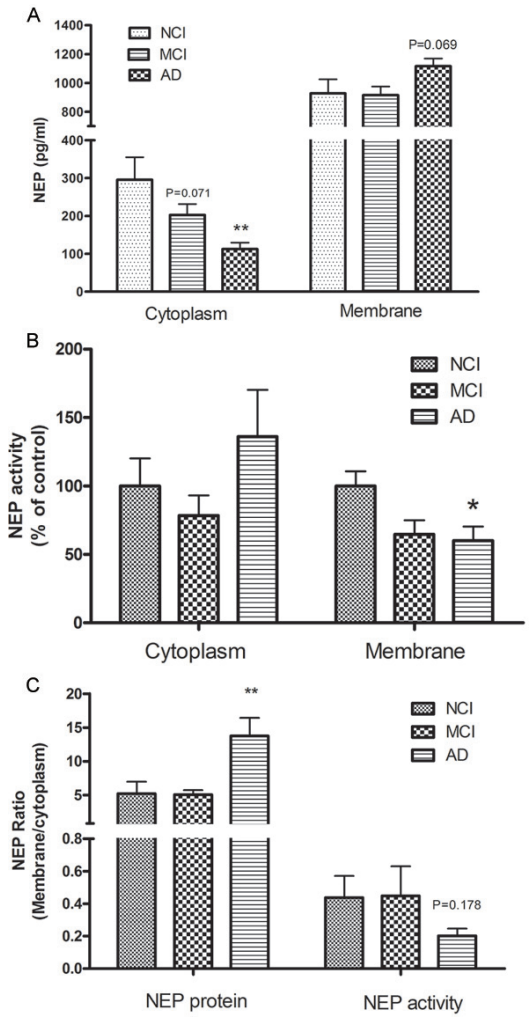

Figure 3. Alterations of NEP membrane/cytoplasmic ratio for protein and enzymatic activity in NCI, MCI and AD. The subcellular fractions of cortical tissues from NCI, MCI and AD brains were prepared for NEP ELISA and activity assays. A: Cytoplasmic and membrane NEP protein levels; B: Cytoplasmic and membrane NEP activity; C: The membrane/cytoplasmic ratio of NEP protein and activity. The data are expressed as mean ± SEM. *$p < 0.05$, **$p < 0.01$ vs NCI control.

Multiple immunohistochemistry and analysis with spectra imaging

Paraffin embedded frontal cortex tissue sections mounted on glass slides from NCI, MCI and AD or from control C56 WT mice and various ages of transgenic APP/PS1 mice were taken through deparaffinization and rehydration. Slides were blocked with endogenous peroxidase blocking buffer (Peroxidazed, Biocare Medical LLC), protein blocking buffer, and alternative antigen retrieval. For multiple labeling, the primary antibodies were applied as a cocktail (rat anti-NEP (15 μg/ml, R&D), rabbit anti-pan-cadherin (1:500, Abcam) in antibody diluent (Renoir Red, Biocare Medical, LLC) overnight at 4°C. Sections were washed with TBS and then incubated with goat anti-mouse HRP polymer for 30 minutes at room temp and goat anti-rabbit AP polymer (Mach 2 Rabbit AP-Polymer) for 60 minutes at room temp. Immunoreactivity was visualized with brown chromogen (Betazoid DAB Chromogen Kit) and red chromogen (Warp Red Chromogen Kit Biocare Medical, LLC) for 7 minutes. After rinsing thoroughly with distilled water, antibodies were denatured (Denaturing Solution Kit Biocare Medical, LLC) for 3 minutes. The third primary antibody was applied (mouse anti NeuN, 1:200, EnCor Biotechnology) in Renoir Red diluent for 60 minutes at room temp. After washing, goat anti-mouse HRP polymer was applied for 30 minutes at room temp. The third chromogen (Vina Green Chromogen Kit, Biocare Medical, LLC) was incubated for 10 minutes. Slides were counterstained with hematoxylin, rinsed with distilled water, dehydrated through graded alcohols and cleared in zylene and coverslipped. The slides were quantitatively analyzed using art imaging systems Vectra™ or Nuance™ (Caliper Life Sciences, Inc, Hopkinton, MA). By using a spectral library, co-localized signals from different antibodies were unmixed and quantified and selecting regions of interest (ROI) for analysis.

Thioflavin-S staining

Senile plaques were detected using thioflavine-S staining according to Wesley Farros' method [37]. Brifely, 40 μm sections were incubated with 0.05% thioflavine-S for 8 minutes, and washed twice in 80% ethanol and water, respectively. The green fluorescence–stained plaques were visualized using fluorescence microscopy. Thioflavine-S positive staining was measured and quantified by Image J.

Statistical analysis

All data were expressed as mean ± standard error of the mean (SEM). Statistical analyses were performed with One-way ANOVA followed by least significant difference post hoc analysis (multiple comparisons) and liner regress analysis with threshold of $P < 0.05$: *$p < 0.05$ and **$p < 0.01$.

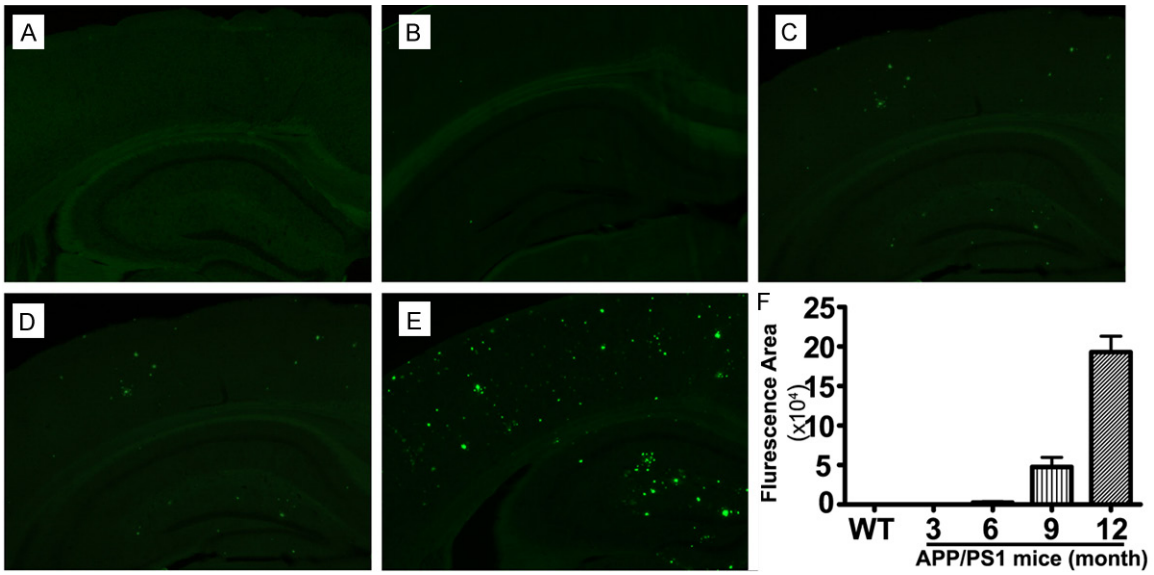

Figure 4. Thioflavine-S staining of brain slices from different months of APP/PS1 and WT mice. A-E: Represents the sections of WT and APP/PS1 transgenic mice of 3, 6, 9 and 12 month, respectively. F: Total fluorescent area measured and quantified by Image J analysis for each group.

Results

Subcellular pattern of NEP in NCI, MCI and AD brains

Multiple immunohistochemical staining of cortical tissue from NCI, MCI and AD, as well as APP/PS1 transgenic mice were used to simultaneously measure NEP, NeuN and pan-cadherin protein and their cellular distribution with a digital imaging system (Vectra™ or Nuance™). **Figure 1A** shows representative captured images using the Nuance™ system. As shown in **Figure 1**, cortical NEP immunoreactivity in MCI was higher compared to NCI, but there was no difference between NCI and AD (**Figure 1B**). Immunoreactivity of the neuronal marker NeuN was lower in MCI and AD, consistent with greater neuronal loss in MCI and AD compared with NCI as shown in previous studies (**Figure 2C**). No changes in the pan-cadherin were observed (**Figure 2D**). Correlation analysis did not find a relation between NEP and NeuN immunoreactivity levels in cortex of NCI and AD, but NEP was negatively correlated with NeuN in MCI ($p < 0.0001$). There was a positive correlation between NEP and pan-cadherin immunoreactivities in NCI and MCI ($P < 0.01$) (**Figure 2**), but not in AD (**Figure 2**).

Using NEP ELISA assays to measure protein level and immunocapture followed by enzyme assay with fluorogenic substrate to specifically measure NEP activity, we measured NEP in subcellular fractions from frontal cortex of NCI, MCI and AD. NEP protein was decreased in MCI and AD cytoplasmic fractions compared with NCI, but NEP protein was increased in the membrane fractions of AD compared with MCI and NCI (**Figure 3A**). The ratio of membrane/cytoplasmic NEP protein was significantly increased in AD (**Figure 3C**). The enzymatic activity of NEP did not follow the same trends noted for protein. In contrast to increases in NEP protein in membrane fractions, the NEP enzyme activity was significantly decreased in the same fractions (**Figure 3B**). The ratio of membrane/cytoplasmic for NEP activity tended to be less, but the difference did not reach statistical significance ($P = 0.178$) (**Figure 3C**).

Amyloid plaque burden staining and subcellular pattern of cortical NEP in the APP/PS1 transgenic mice

Transgenic mice have proven to be a valuable model system to study pathological features shared with AD such as Aβ deposition. In this study, we measured NEP protein and enzyme activity in APP/PS1 mice at time points (3 months) before amyloid plaques are detected but at which time intraneuronal accumulation of Aβ is detected in hippocampus and cortex (**Figure 4B**, **4F**), as well as at time points (6

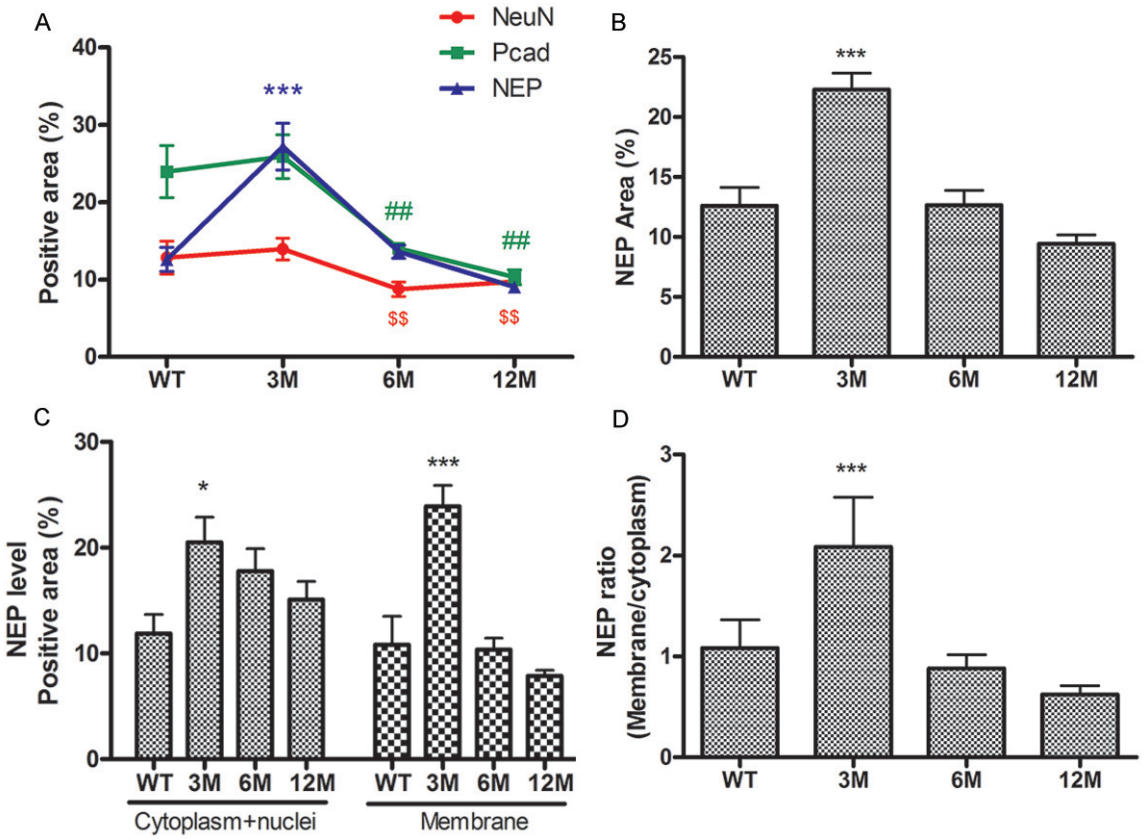

Figure 5. Alteration of cortical NEP levels in APP/PS1 transgenic mice. Brain slides from C57 WT mice and various ages of transgenic APP/PS1 were immunostained for NEP, NeuN and pan-cadherin following by quantitative analysis using Art Imaging Systems Nuance™. A: Total positive pixel area for NEP, NeuN and pan-cadherin in mice at 3, 6, 9 and 12 months of age. B: Total NEP positive area; C: Membrane/cytoplasmic NEP positive area; D: NEP membrane/cytoplasm ratio. The data are expressed as mean ± SEM. *p < 0.05, **p < 0.01 vs WT control.

months) when plaques are prevalent (**Figure 4C**, **4F**). Compared to controls, NEP immunoreactivity was increased at 3 months (similar to findings in humans with MCI) and then decreased after 6 months (similar to humans with AD) (**Figure 5A**, **5B**). NeuN and pan-cadherin decreased after 6 months (similar to patterns noted in MCI and AD) (**Figure 5A**).

Analysis of NEP in subcellular fractions showed that both cytoplasmic and membrane fractions had increased NEP at 3 months and decreased NEP after 6 months of age. The changes were most marked for membrane compared with cytoplasmic NEP (**Figure 5C**). Thus, the ratio of membrane/cytoplasmic NEP was significantly increased in 3 months mice (**Figure 5D**). While there are no obvious Aβ deposits at 3 months (**Figure 4**), when NEP is decreased in terms of both protein levels and enzyme activity after this time point, the decreases in NEP are associated with increasing Aβ accumulation in extracellular deposits in the brain.

The subcellular profile of NEP in Aβ and HNE-treated neuroblastoma SH-SY5Y cells

Treatment of human neuroblastoma SH-SY5Y cells with Aβ or an inducer of oxidative stress, HNE, produced up-regulation of NEP beginning at 24 hours and persisting to 72 hours. Protein levels of NEP in both cytoplasmic and membrane fractions increased, with the most marked increases in cytoplasmic fractions (**Figure 6A**, **6B**). In contrast to changes in protein level, NEP enzyme activity was decreased in cytoplasmic fractions in cells exposed to Aβ and HNE at 24 and 72 hours. The activity of membrane NEP increased at 48 hours and then significantly decreased (**Figure 6C**, **6D**). The ratios of cytoplasmic/membrane NEP protein and activity ratios calculated at the three

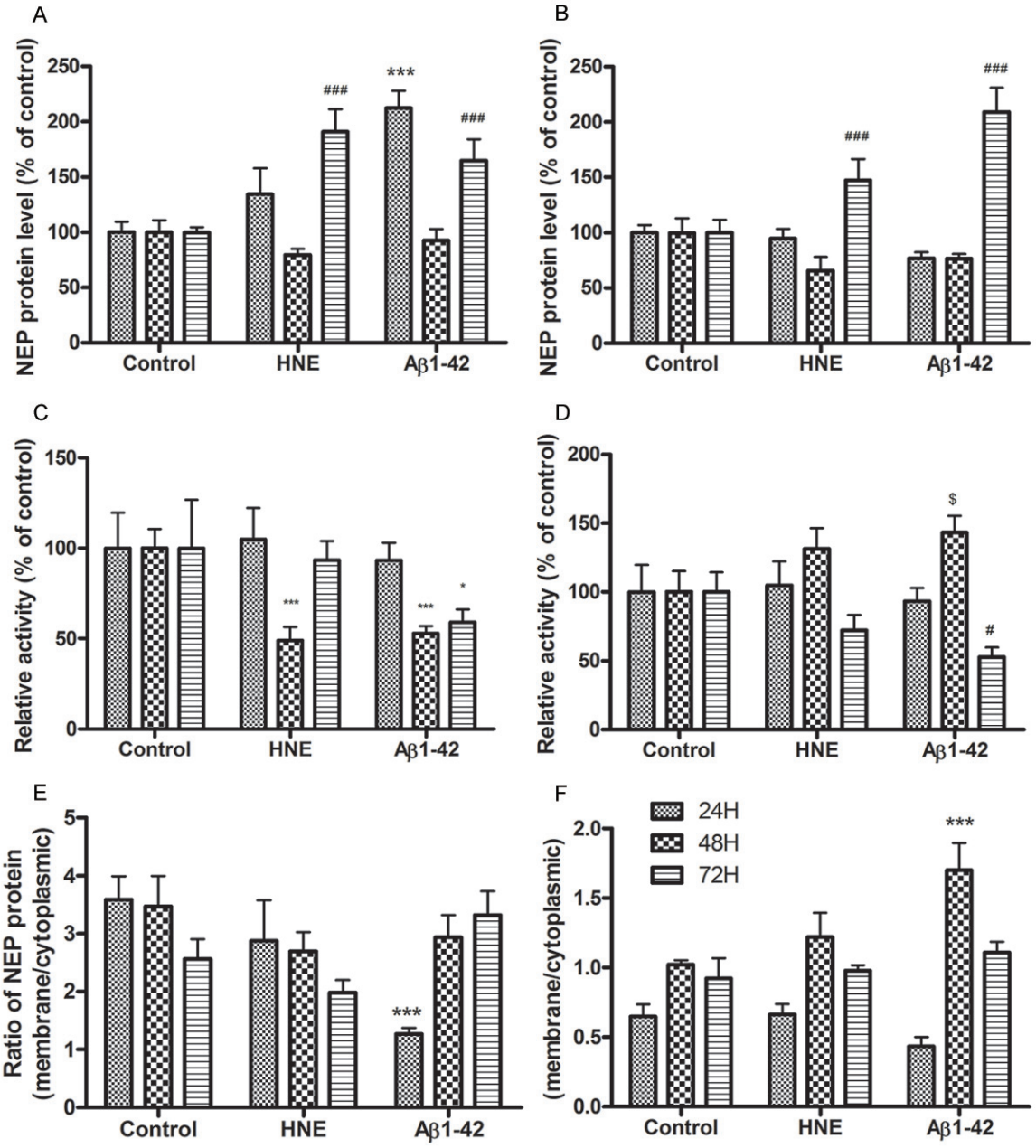

Figure 6. Alteration of cytoplasmic and membrane NEP protein and activity in HNE and Aβ1-42 treated SH-SY5Y cells. Different concentrations of HNE or Aβ were added to the cultures 24-72 h before harvest. The membrane and cytoplasm fractionations were extracted for the determination of NEP protein and activity. A and C: Cytoplasmic NEP protein and activity, respectively; B and D: Membrane NEP protein and activity, respectively. E and F: The membrane/cytoplasmic ration of NEP protein and activity.

time points showed marked increases in NEP protein at 24 hours, then decreases at 48 and 72 hours for both Aβ and HNE treated cells (**Figure 6E**). These results suggest that oxidative stress and exogenous Aβ lead to up-regulation of NEP protein expression; however, the ratio of NEP enzyme activities did not show comparable changes (**Figure 6F**). The latter may indicate that the major NEP enzyme activity is associated with membrane rather than cytoplasmic fractions.

Discussion

In addition to dysregulated production, increasing experimental evidence suggests reduced

catabolism also plays an important role in Aβ accumulation. We have previously shown that NEP is modified by 4-hydroxy-nonenal (HNE) adducts in the brain of persons with AD [38] and in human neuroblastoma treated with either HNE or Aβ [35, 39]. The *in vitro* study revealed that HNE-modified NEP had decreased catalytic activity that was associated with elevations in Aβ1-40. That study also showed Aβ treatment induced increases in NEP protein with a lower catabolic activity, which might demonstrate an compensatory response to the decreased activity of NEP due to HNE-adduct formation [35]. It has been shown that Aβ has a very high clearance rate in the human central nervous system (CNS) [40]. This high clearance rate may be achieved by the presence of cryptidases, including NEP, in multiple cellular compartments. Despite a large number of cell biological studies of Aβ metabolism and transport, it still remains unclear exactly how Aβ is cleared in neurons, especially in specific cellular compartments and how it changes during the evolution of AD. NEP protein and activity were detected in both membrane and cytoplasmic compartments in the present study (**Figures 1** and **2**). It is accepted that the extracellular space is a primary site for Aβ accumulation in the form of amyloid plaques and amyloid angiopathy in aging and AD. Extracellular Aβ can be degraded by cell surface and secreted forms of cryptidases, including NEP and insulin degrading enzyme (IDE) [40, 41]. As expected, NEP protein was lower in MCI and AD cytoplasmic fractions, but elevated in the membrane fraction, with a significant increase of the membrane/cytoplasmic ratio of NEP protein in AD (**Figure 1A**, **1C**). On the other hand, NEP enzyme activity was lower (**Figure 1B**, **1C**), consistent with our previous study [35, 39].

The present study also demonstrated that NeuN, a neuronal marker, was lower in both MCI and AD, suggesting detectable neuronal loss in MCI as well as in AD. The result is consistent with previous studies [21, 25, 35, 39]. However, we did not find a correlation between NEP and NeuN in NCI and AD, but an inverse correlation in MCI brains ($p < 0.0001$). The result might indicate an increased NEP expression in non-neuronal cells, such as astrocytes and microglia. We found that GFAP, an astrocyte marker, was lower in both MCI and AD. Meanwhile, Iba1, an activated microglia marker, was elevated in MCI and AD brains. GFAP was inversely correlated with NEP significantly both in NCI and MCI, but positively correlated in AD. We did not find a correlation between Iba1 and NEP in MCI and AD, but they were correlated in NCI brains (unpublished data). Those findings provide some evidence to support the hypothesis above. Cadherin proteins are integral to the plasma membrane and function in cellular adhesion, in both tissues and cultured cells. Classical cadherin, including N-cadherin, E-cadherin, and VE-cadherin, feature a 24-amino acid sequence in the carboxy terminal that is conserved among cadherin family proteins and across animal species. Since cadherin expression and localization is intimately related to cell adhesion, antibodies generated against the 24-amino acid sequence, termed "pan-cadherin", was used as a marker of cytoplasmic membrane. The level of pan-cadherin immunoreactivity was not different between NCI, MCI or AD, but there was a trend for it to be higher in AD. NEP positively correlated to pan-cadherin in NCI and MCI cortex, which might imply an important role of membrane-bond NEP in Aβ degradation in NCI and MCI brain, as seen in previous studies [34, 42]. No association between NEP and pan-cadherin in AD might indicate be related to the greater proportion of NEP in cytoplasmic than membrane compartment.

Previous studies have shown that NEP is primarily located at the cell surface [43], and Fukami et al. showed both synaptic and axonal localization of NEP in hippocampal and neocortical neurons [44]. Degradation of Aβ by NEP is thought to occur at or near synapses and inside secretory vesicles during axonal transport. Neprilysin is likely to influence the local concentrations of Aβ at least in the extracellular space close to synapses, possibly affecting the local pathology during the course of AD. The results of the present study suggest that the subcellular distribution of NEP protein and enzyme activity were altered in different stages of AD development. In particular, we observed lower cytoplasmic NEP protein in MCI and AD compared to NCI, while membrane associated NEP protein tended to be higher in AD. By contrast, the subcellular distribution of NEP enzyme activity was inverse as shown by membrane/cytoplasm ratio. We found lower NEP activity in the membrane compartment in AD (**Figure 3C**). These data provide more evidence to support findings from our previous study in which we

demonstrated that NEP in AD brain tissue is modified through HNE adducts and that similar changes are observed in NEP in both HNE- and Aβ-treated neuronal cell lines. The HNE modification of NEP may be an important factor in decreasing NEP catalytic activity in AD [35, 39]. The shift of NEP from cytoplasmic to membrane compartments may be a compensation for decreases in activity in membrane associated NEP in AD. This hypothesis is supported by finding increased membrane/cytoplasm NEP ratio in APP/PS1-transgenic mice at 3 months of age prior to amyloid deposition, which decreased after 3 months as amyloid deposits increased (**Figure 4D**).

Additional studies in human neuroblastoma SH-SY5Y cells showed acute changes in NEP induced by exogenous HNE and Aβ, with up-regulation of NEP protein by both agents, initially in the cytoplasm compartment, which is in accord with the expected pattern for a newly synthesized enzyme. The decreased NEP activity in cytoplasmic fractions in HNE and Aβ treated cells may suggest that some NEP in this compartment is immature and less enzymatically active, although it is also possible that other regulatory mechanisms may be involved. By expressing NEP chimeric proteins containing various subcellular compartment-targeting domains in neurons, Hama et al. showed that different intracellular compartments may be involved in the metabolism of distinct pools of Aβ (Aβ40 and Aβ42) that may be retained or recycled intracellularly or secreted extracellularly, and that endogenous targeting of wild-type NEP is optimized for the overall neuronal clearance of Aβ [34].

The mitogen-activated protein kinases/extracellular signal-regulated kinases (MEK/ERK) pathway is a part of a signal transduction pathway in cells that communicates a signal from a receptor on the cell surface to transcriptional changes in the nucleus. There are multiple lines of evidence suggesting that the MEK/ERK pathways activation is involved in AD [45]. For example, MEK signaling is increased in vulnerable neurons and linked to abnormal phosphorylation of cytoskeletal proteins in AD [46]. Aβ peptide can directly trigger multiple intracellular signaling pathways, including the MEK/ERK pathway [47]. It has been suggested that neurotrophic factors, such as brain-derived neurotrophic factor, nerve growth factor and neurotrophins 3 and 4, can reduce cell surface NEP activity [42]. This decrease is mediated by MEK/ERK signaling, which enhanced phosphorylation at serine 6 in the NEP intracellular domain. Increased phosphorylation of serine-6 of NEP in primary neurons has been shown to reduce the levels of cell surface NEP, which leads to increases in extracellular Aβ. These studies indicate that phosphorylation of serine-6 of NEP influences the subcellular localization of NEP and that this affects extracellular Aβ levels [42].

Given the crucial role that membrane-bond NEP plays in Aβ metabolism and clearance, together with the aberrant NEP expression/activity relationship observed in the present stud in different cell compartments of AD brain, it is reasonable to propose that aberrant localization and modulation of NEP activity might participate in the decreased Aβ degradation that is a critical component of AD pathogenesis that manifests in extracellular deposits of Aβ in senile plaques and amyloid angiopathy in AD.

Acknowledgements

This work was supported by the grants to Rui Wang from National Natural Science Foundation of China (81072627); Pujiang talent project of Shanghai (11PJ1402300); Shanghai Committee of Science and Technology (11DZ2260600); 111 Project (Grant No. B07023) and the grants to Dengshun Wang from National Institutes of Health (NIH) grants AG025722 and AG029972, and an Alzheimer's Association grant IIRG-08-90524. The human samples used in this study are from NIH grants to David Bennett (P30AG10161, R01AG15819).

Address correspondence to: Dr. Rui Wang, Shanghai Key Laboratory of New Drug Design, School of Pharmacy, East China University of Science and Technology, 130 Meilong Road, Shanghai 200237, China. Tel: +86-21-64250823; Fax: +86-21-64250823; E-mail: ruiwang@ecust.edu.cn; Dr. Dengshun Wang, 1300 University Avenue, Madison, WI 53706, USA. Tel: +1-608-262-9825; Fax: +1-608-265-3301; E-mail: dwang6@wisc.edu

References

[1] Selkoe DJ. Aging, amyloid, and Alzheimer's disease: A perspective in honor of Carl Cotman. Neurochem Res 2003; 28: 1705-1713.

[2] Brown J, Smith S, Brun A, Collinge J, Gydesen S, Hardy J, Mullan M and Goate A. Genetic characterization of a novel familial dementia. Ann N Y Acad Sci 1991; 640: 181-183.
[3] Goate A, Chartier-Harlin MC, Mullan M, Brown J, Crawford F, Fidani L, Giuffra L, Haynes A, Irving N, James L, et al. Segregation of a missense mutation in the amyloid precursor protein gene with familial Alzheimer's disease. Nature 1991; 349: 704-706.
[4] Sherrington R, Rogaev EI, Liang Y, Rogaeva EA, Levesque G, Ikeda M, Chi H, Lin C, Li G, Holman K, Tsuda T, Mar L, Foncin JF, Bruni AC, Montesi MP, Sorbi S, Rainero I, Pinessi L, Nee L, Chumakov I, Pollen D, Brookes A, Sanseau P, Polinsky RJ, Wasco W, Da Silva HAR, Haines JL, Pericak-Vance MA, Tanzi RE, Roses AD, Fraser PE, Rommens JM and St George-Hyslop PH. Cloning of gene bearing missense mutations in early-onset familial Alzheimer's disease. Nature 1995; 375: 754-760.
[5] Levy-Lahad E, Wasco W, Poorkaj P, Romano DM, Oshima J, Pettingell WH, Yu CE, Jondro PD, Schmidt SD, Wang K, Crowley AC, Fu YH, Guenette SY, Galas D, Nemens E, Wijsman EM, Bird TD, Schellenberg GD and Tanzi RE. Candidate gene for the chromosome 1 familial Alzheimer's disease locus. Science 1995; 269: 973-977.
[6] Jayadev S, Leverenz JB, Steinbart E, Stahl J, Klunk W, Yu CE and Bird TD. Alzheimer's disease phenotypes and genotypes associated with mutations in presenilin 2. Brain 2010; 133: 1143-1154.
[7] Iwata N, Tsubuki S, Takaki Y, Shirotani K, Lu B, Gerard NP, Gerard C, Hama E, Lee HJ and Saido TC. Metabolic regulation of brain A beta by neprilysin. Science 2001; 292: 1550-1552.
[8] Roques BP, Fournie-Zaluski MC, Soroca E, Lecomte JM, Malfroy B, Llorens C and Schwartz JC. The enkephalinase inhibitor thiorphan shows antinociceptive activity in mice. Nature 1980; 288: 286-288.
[9] Roques BP, Garbay-Jaureguiberry C, Bajusz S and Maigret B. Studies of the conformational behaviour and preferential interactions with opiate receptors of the cis and trans forms of Dmet2,pro5 enkephalin and Dmet2,pro5 enkephalinamide by 1H and 13C NMR, theoretical calculations and 13C relaxation measurements. Eur J Biochem 1980; 113: 105-119.
[10] Fulcher IS, Matsas R, Turner AJ and Kenny AJ. Kidney neutral endopeptidase and the hydrolysis of enkephalin by synaptic membranes show similar sensitivity to inhibitors. Biochem J 1982; 203: 519-522.
[11] Matsas R, Fulcher IS, Kenny AJ and Turner AJ. Substance P and Leu enkephalin are hydrolyzed by an enzyme in pig caudate synaptic membranes that is identical with the endopeptidase of kidney microvilli. Proc Natl Acad Sci U S A 1983; 80: 3111-3115.
[12] Eckman EA, Adams SK, Troendle FJ, Stodola BA, Kahn MA, Fauq AH, Xiao HD, Bernstein KE and Eckman CB. Regulation of steady-state beta-amyloid levels in the brain by neprilysin and endothelin-converting enzyme but not angiotensin-converting enzyme. J Biol Chem 2006; 281: 30471-30478.
[13] Miners JS, Barua N, Kehoe PG, Gill S and Love S. A beta-Degrading Enzymes: Potential for Treatment of Alzheimer Disease. J Neuropathol Exp Neurol 2011; 70: 944-959.
[14] Mouri A, Zou LB, Iwata N, Saido TC, Wang DY, Wang MW, Noda Y and Nabeshima T. Inhibition of neprilysin by thiorphan (i.c.v.) causes an accumulation of amyloid beta and impairment of learning and memory. Behav Brain Res 2006; 168: 83-91.
[15] Zou LB, Mouri A, Iwata N, Saido TC, Wang DY, Wang MW, Mizoguchi H, Noda Y and Nabeshima T. Inhibition of neprilysin by infusion of thiorphan into the hippocampus causes an accumulation of amyloid beta and impairment of learning and memory. J Pharmacol Exp Ther 2006; 317: 334-340.
[16] Iwata N, Mizukami H, Shirotani K, Takaki Y, Muramatsu S, Ozawa K and Saido TC. A possibility of gene therapy for Alzheimer's disease by neprilysin gene transfer. Neurobiology of Aging 2004; 25: S590-S590.
[17] Liu Y, Studzinski C, Beckett T, Guan H, Hersh MA, Murphy MP, Klein R and Hersh LB. Expression of Neprilysin in Skeletal Muscle Reduces Amyloid Burden in a Transgenic Mouse Model of Alzheimer Disease. Mol Ther 2009; 17: 1381-1386.
[18] El-Amouri SS, Zhu H, Yu J, Gage FH, Verma IM and Kindy MS. Neprilysin protects neurons against A beta peptide toxicity. Brain Res 2007; 1152: 191-200.
[19] Yoon SS and Jo SA. Mechanisms of Amyloid-beta Peptide Clearance: Potential Therapeutic Targets for Alzheimer's Disease. Biomolecules & Therapeutics 2012; 20: 245-255.
[20] Yang HQ and Xing Y. Role of Neprilysin in The Pathogenesis of Alzheimer's Disease. Progress in Biochemistry and Biophysics 2012; 39: 721-725.
[21] Wang DS, Lipton RB, Katz MJ, Davies P, Buschke H, Kuslansky G, Verghese J, Younkin SG, Eckman C and Dickson DW. Decreased neprilysin immunoreactivity in Alzheimer disease, but not in pathological aging. J Neuropathol Exp Neurol 2005; 64: 378-385.
[22] Wang JY, Ohno-Matsui K and Morita I. Elevated amyloid beta production in senescent retinal pigment epithelium, a possible mechanism of

subretinal deposition of amyloid beta in age-related macular degeneration. Biochem Biophys Res Commun 2012; 423: 73-78.
[23] Barua NU, Miners JS, Bienemann AS, Wyatt MJ, Welser K, Tabor AB, Hailes HC, Love S and Gill SS. Convection-Enhanced Delivery of Neprilysin: A Novel Amyloid-beta-Degrading Therapeutic Strategy. J Alzheimers Dis 2012; 32: 43-56.
[24] Proctor CJ, Pienaar IS, Elson JL and Kirkwood TBL. Aggregation, impaired degradation and immunization targeting of amyloid-beta dimers in Alzheimer's disease: a stochastic modelling approach. Mol Neurodegener 2012; 7: 32.
[25] Wang DS, Dickson DW and Malter JS. beta-amyloid degradation and Alzheimer's disease. J Biomed Biotechnol 2006; 2006: 58406.
[26] Wang S, Wang R, Chen L, Bennett DA, Dickson DW and Wang DS. Expression and functional profiling of neprilysin, insulin-degrading enzyme, and endothelin-converting enzyme in prospectively studied elderly and Alzheimer's brain. J Neurochem 2010; 115: 47-57.
[27] Turner AJ and Tanzawa K. Mammalian membrane metallopeptidases: NEP, ECE, KELL, and PEX. FASEB J 1997; 11: 355-364.
[28] Sato K, Tanabe C, Yonemura Y, Watahiki H, Zhao Y, Yagishita S, Ebina M, Suo S, Futai E, Murata M and Ishiura S. Localization of Mature Neprilysin in Lipid Rafts. J Neurosci Res 2012; 90: 870-877.
[29] Kawarabayashi T, Shoji M, Wahrle S, Younkin LH and Younkin SG. Amyloid beta protein accumulates in lipid rafts. Society for Neuroscience Abstracts 2001; 27: 1518-1518.
[30] Takaki Y, Tsubuki S, Iwata N, Shirotani K, Yano L, Okamoto T, Gerard N, Lu B, Gerard C and Saido TC. Association of Abeta-metabolizing neutral endopeptidases with lipid raft in the brain. Society for Neuroscience Abstracts 2001; 27: 1519-1519.
[31] Cordy JM, Hooper NM and Turner AJ. The involvement of lipid rafts in Alzheimer's disease (Review). Mol Membr Biol 2006; 23: 111-122.
[32] Turner AJ, Sims C, Cordy JM, Thornhill P, Fisk L and Nalivaeva NN. Dynamics of amyloid metabolism: the role of cholesterol, lipid rafts and hypoxia in amyloidogenesis. Journal of Neurochemistry 2006; 99: 30-31.
[33] Hama E, Shirotani K, Masumoto H, Sekine-Aizawa Y, Aizawa H and Saido TC. Clearance of extracellular and cell-associated amyloid beta peptide through viral expression of neprilysin in primary neurons. J Biochem 2001; 130: 721-726.
[34] Hama E, Shirotani K, Iwata N and Saido TC. Effects of neprilysin chimeric proteins targeted to subcellular compartments on amyloid beta peptide clearance in primary neurons. J Biol Chem 2004; 279: 30259-30264.
[35] Wang R, Wang S, Malter JS and Wang DS. Effects of HNE-modification induced by A beta on neprilysin expression and activity in SH-SY5Y cells. J Neurochem 2009; 108: 1072-1082.
[36] Bennett DA, Schneider JA, Arvanitakis Z and Wilson RS. Overview and findings from the religious orders study. Curr Alzheimer Res 2012; 9: 628-645.
[37] Farris W, Schütz SG, Cirrito JR, Shankar GM, Sun X, George A, Leissring MA, Walsh DM, Qiu WQ, Holtzman DM, Selkoe DJ. Loss of Neprilysin Function Promotes Amyloid Plaque Formation and Causes Cerebral Amyloid Angiopathy. Am J Pathol 2007; 171: 241-251.
[38] Wang DS, Iwata N, Hama E, Saido TC and Dickson K. Oxidized neprilysin in aging and Alzheimer's disease brains. Biochem Biophys Res Commun 2003; 310: 236-241.
[39] Wang R, Malter JS and Wang DS. N-Acetylcysteine Prevents 4-Hydroxynonenal- and Amyloid-beta-Induced Modification and Inactivation of Neprilysin in SH-SY5Y Cells. J Alzheimers Dis 2010; 19: 179-189.
[40] Nalivaeva NN, Beckett C, Belyaev ND and Turner AJ. Are amyloid-degrading enzymes viable therapeutic targets in Alzheimer's disease? J Neurochem 2012; 120: 167-185.
[41] Kraemer HH, He L, Lu B, Birklein F and Sommer C. Increased pain and neurogenic inflammation in mice deficient of neutral endopeptidase. Neurobiol Dis 2009; 35: 177-183.
[42] Kakiya N, Saito T, Nilsson P, Matsuba Y, Tsubuki S, Takei N, Nawa H and Saido TC. Cell Surface Expression of the Major Amyloid-beta Peptide (A beta)-degrading Enzyme, Neprilysin, Depends on Phosphorylation by Mitogen-activated Protein Kinase/Extracellular Signal-regulated Kinase Kinase (MEK) and Dephosphorylation by Protein Phosphatase 1a. J Biol Chem 2012; 287: 29362-29372.
[43] Shirotani K, Tsubuki S, Iwata N, Takaki Y, Harigaya W, Maruyama K, Kiryu-Seo S, Kiyama H, Iwata H, Tomita T, Iwatsubo T and Saido TC. Neprilysin degrades both amyloid beta peptides 1-40 and 1-42 most rapidly and efficiently among thiorphan- and phosphoramidon-sensitive endopeptidases. J Biol Chem 2001; 276: 21895-21901.
[44] Fukami S, Watanabe K, Iwata N, Haraoka J, Lu B, Gerard NP, Gerard C, Fraser P, Westaway D, St George-Hyslop P and Saido TC. A beta-degrading endopeptidase, neprilysin, in mouse brain: synaptic and axonal localization inversely correlating with A beta pathology. Neurosci Res 2002; 43: 39-56.
[45] Haddad JJ. Mitogen-activated protein kinases and the evolution of Alzheimer's: a revolutionary neurogenetic axis for therapeutic intervention? Prog Neurobiol 2004; 73: 359-377.

[46] Wong J, Higgins M, Halliday G and Garner B. Amyloid beta selectively modulates neuronal TrkB alternative transcript expression with implications for Alzheimer's disease. Neuroscience 2012; 210: 363-374.
[47] Fu W, Ruangkittisakul A, MacTavish D, Shi JY, Ballanyi K and Jhamandas JH. Amyloid beta (A beta) Peptide Directly Activates Amylin-3 Receptor Subtype by Triggering Multiple Intracellular Signaling Pathways. J Biol Chem 2012; 287: 18820-18830.